Acta Sci. Pol.
Formatio Circumiectus 17 (4) 2018, 69–84
ENVIRONMENTAL PROCESSES

www.formatiocircumiectus.actapol.net/pl/ ISSN 1644-0765 DOI:

ORIGINAL PAPER Accepted:

APPLYING LASER SCANNING TECHNOLOGY TO STUDYING ALLUVIAL FLUME-BED TOPOGRAPHY IN LABORATORY CONDITIONS

Marta Kiraga[1]✉, Mateusz Razumnik[2], Zbigniew Popek[1], Leszek Chmielewski[2]

[1] Department of Civil Engineering, Faculty of Civil and Environmental Engineering, Warsaw University of Life Sciences, ul. Nowoursynowska 159, 02-776 Warsaw, e-mail: marta_kiraga@sggw.pl
[2] Department of Informatics, Faculty of Applied Informatics and Mathematics, Warsaw University of Life Sciences, ul. Nowoursynowska 159, 02-776 Warsaw

ABSTRACT

The aim of the research was to compare alluvial bed topography description in laboratory conditions using the "traditional", currently applicable method with an original approach, based on LiDAR technology.

LiDAR application in local scours shape investigation in based on the grounds of introducing the autonomic measuring module, which, placed above the bed on dedicated controllable arrangement of guideways, describes the landform as a cloud of coordinates.

The result of the performed experiment was obtainment of point clouds (x, y, z), reflecting the bed shape before and after local scour formation during twenty measurement series with varying hydraulic conditions. Objects of the study were basic geometry properties of the scour hole and its volume. The measurement with laser scanner technology application allowed for obtaining much more accurate results in shorter time, comparison to disc probe survey, and also relatively fast conversion of numerical data into figures. The device equipped with portable computer, precise stepper motors and dedicated software permitted the introduction of automation into laboratory work. The effect is not only measurements accuracy, but also significant acceleration of data gathering. The adopted grid is characterized by significant density, which – in connection with meaningfully high accuracy – allows very precise surface description. Bed shape can be presented in numerical or graphical form. It must be pointed out that disc probe method application would never give such accuracy as in the case of introducing laser scanning technology in similar studies.

Keywords: laser scanning, surface interpolation, local scouring, bed measurements, water structures

INTRODUCTION

Due to the partition of the river with a damming structure, stability of the riverbed is disturbed, and two different areas are created, with different bed load transport conditions. The morphological changes resulting from the damming of the river concern both the lower and upper stations. On the top station of the structure, as a result of water accumulation, a weir-adjoining channel or valley reservoir is formed, in which, due to the decrease of the water flow velocity, sedimentation and accumulation occurs of initially thicker, then fine debris particles (see: Fig. 1). Part of the bed load may thus be stopped in the upper station. On the other hand, below the obstacle, the stream of water acquires more energy as a result of accumulation, which with total or partial lack of bed load transport from the upper station causes downcutting or bottom erosion of the river bed in the lower station.

✉e-mail: marta_kiraga@sggw.pl

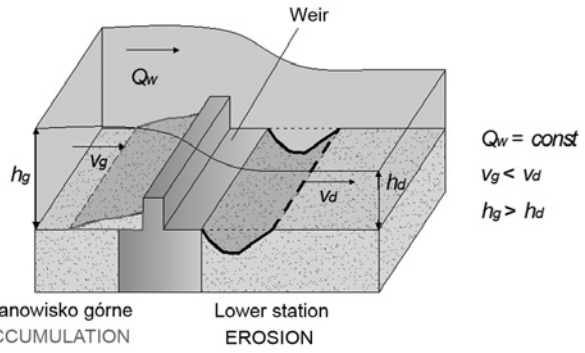

Fig. 1. Morphological changes resulting from damming the river bed with a hydraulic structure, in this case a weir, where: Q_w – water flow, v_g, v_d – average water velocity in the upper and lower station of the structure h_g, h_d – water depth in = the upper and lower station of the structure, W – width of the river bed

The erosive processes of the lower station of the structure are permanent, and they cover an increasingly longer section of the river (Wierzbicki and Hämmerling, 2011). Local lateral erosion can deepen, depending on the hydrodynamic conditions. Especially dangerous are the catastrophic flood freshets, during which the resulting pothole in the river bottom of the lower station may threaten the stability of the structure (Clarke, 1962; Kaszowski et al., 1970; Petts, 1977; Bajkowski et al., 2002).

Undertaken studies and analyses of the formation of local lateral erosion in various conditions of hydrotechnical structures testify to the complex course of the phenomenon, which poses difficulties in its description and analysis of the obtained results (Lenzi et al., 2003; Pagliara et al., 2017). So far, no theoretical basis for the creation of local lateral erosion of riverbed has been formulated, which prompts the need for further empirical studies of the phenomenon. Significant difficulties encountered especially during field tests result from the complexity of the process of separating and transferring bed load particles of diverse grain size, as well as the lack of accurate data on the shape of the riverbed before the formation of lateral erosion, combined with high uncertainty of field measurement results.

Most attempts to identify and describe the phenomenon of the formation of local pockets of riverbed lateral erosion were carried out in laboratory conditions. Although the results of these studies are difficult to generalize, the obtained empirical formulas are usually of limited application in designing practice (Błażejewski, 1989; Breusers and Raudkivi, 1991; Ślizowski and Radecki-Pawlik, 2003; Urbański, 2005; Ben Meftah and Mossa, 2006; Urbański and Hejduk, 2014; Kiraga and Popek, 2016 a,b; Kiraga and Popek, 2018). On the other hand, it is an important advantage of laboratory tests that it enables us to study the impact of different types of damming structures in a wide range of hydraulic conditions. Furthermore, state-of-the-art measuring equipment can be used more extensively in laboratory conditions (Bajkowski, 2010). However, while the measurements of hydraulic parameters in the laboratory are characterized by high accuracy, the measurement of the shape of the eroded riverbed is still performed using simple devices such as for instance a disc probe or a water level pin gauge.

Many empirical formulas directly associate the hydraulic and granulometric conditions of the bed load with the geometry of the potholes, i.e. the maximum depth or length of the eroded hollow (Chividini, 1983; Gaudio et al., 2000; Lenzi et al., 2003; Ślizowski and Radecki-Pawlik, 2003; Novak et al., 2006; Kiraga and Popek, 2016 a,b, 2017). Therefore, during the research, it is necessary to determine the initial and final shape of the riverbed, which requires time-consuming measurements of the bottom heights in the assumed grid of points – usually with a relatively high density of the "mesh". In the current laboratory tests, blur the bottoms, including those carried out in the Hydraulic Laboratory. In laboratory studies of lateral erosion to date, including the ones conducted by Armand Żbikowski at the Faculty of Civil Engineering and Environmental Engineering at WULS-SGGW, the shape of the bottom was determined on the basis of measurements made using a handheld disc probe (Dąbkowski and Siwicki, 2000; Bajkowski et al., 2002; Urbański, 2005; Kiraga and Popek, 2016 a, b; Kiraga and Popek, 2018). The difficulty associated with the use of this type of device, in addition to the prolonged measurement time, is also the inability to directly obtain the results in the digital format, and automatically save them in a computer or on an electronic medium. In order to eliminate these inconveniences, a measuring device based on

laser scanning technology was constructed, created in 2016–2017 as part of a WULS-SGGW research grant for young scientists.

RESEARCH METHODOLOGY

Comparative studies of the shape of the riverbed, using the traditional method, that is, a disc probe, and using laser scanning technology, were carried out at the WULS-SGGW Hydraulic Laboratory, below the damming structure in the form of a gate valve, within the lower station with a bottom subject to lateral erosion (see: Fig. 2). Twenty test series were carried out in twenty different variations of water level and water flow, within the range of flow rate of Q_w = 0.015–0.045 $m^3 \cdot s^{-1}$ and riverbed filling of h_0 = 0.05–0.20 m. Unit flows $q_w = Q_w/W$ amounted to 0.021–0.052 $m^3 \cdot s^{-1}$ m^{-1}, while the speed of flowing water in the upper station (above the structure) from 0.080 $m^3 \cdot s^{-1}$ to 0.862 $m^3 s^{-1}$ (see: Table 1). Local lateral erosion pockets formed below the gate valve within the sandy riverbed due to the increase of stream energy caused by the increase in the speed of water flowing through the cross-section of the structure (the gate valve was raised to 5 cm of height) and the increase in tangential stress caused by different roughness of the material forming the riverbed. The measurement of the evolution of the riverbed was carried out over time, allowing for the determination of the shape that could be recognized as indicating that the system has reached the state of dynamic equilibrium (Chabert and Engeldinger; 1956). The research was carried out under the conditions of the so-called mobile riverbed,

Table 1. Basic hydraulic parameters of measurement series

No. of measurement series	Q_w [$m^3 \cdot s^{-1}$]	h_g [m]	v_g [$m \cdot s^{-1}$]	q_w [$m^3 \cdot s^{-1} \cdot m^{-1}$]	T_c [s]	T_r [s]
1	0.020	0.13	0.276	0.034	28800	3600
2	0.025	0.13	0.345	0.043	28800	18000
3	0.020	0.05	0.690	0.034	28800	21600
4	0.015	0.10	0.259	0.026	28800	18000
5	0.023	0.10	0.397	0.040	28800	21600
6	0.018	0.10	0.310	0.031	28800	7200
7	0.018	0.15	0.207	0.031	28800	18000
8	0.030	0.08	0.647	0.052	28800	14400
9	0.025	0.05	0.862	0.043	28800	18000
10	0.030	0.11	0.470	0.052	28800	21600
11	0.028	0.11	0.439	0.048	28800	21600
12	0.026	0.10	0.448	0.045	28800	18000
13	0.029	0.08	0.625	0.050	28800	18000
14	0.016	0.23	0.120	0.028	28800	3600
15	0.012	0.26	0.080	0.021	28800	3600
16	0.017	0.16	0.180	0.029	28800	3600
17	0.024	0.08	0.500	0.041	28800	21600
18	0.013	0.25	0.090	0.022	28800	3600
19	0.020	0.11	0.300	0.034	28800	21600
20	0.029	0.10	0.500	0.050	28800	14400

where: Q_w – flow rate, h_g – water depth in the station of the structure, v_g – average water velocity in the upper station of the structure, q_w – unit flow rate (stream flow), T_c – total duration of the measurement duration T_r – time of the shaping of lateral erosion

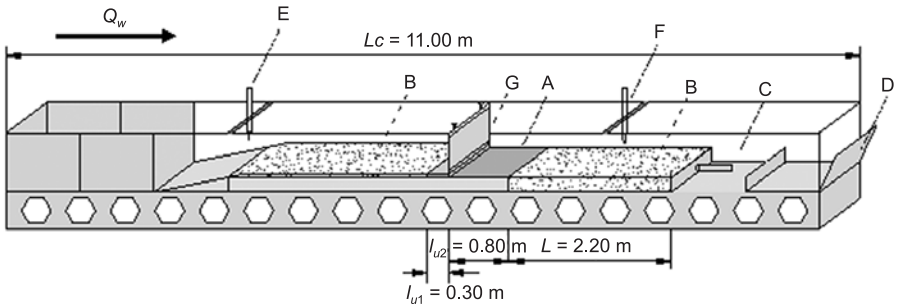

Fig. 2. Schematic of laboratory through (all measurements in metres), where: Q_w – flow rate with the indication of the direction of flow; *A* – riverbed not subjected to lateral erosion; *B* – riverbed subjected to lateral erosion; *C*– collector chamber; *D* – control valve; *E* – water level pin gauge; *F* – disc probe with adjustable water gauge; *G* – gate valve with bottom reinforcements; L_c – total length of laboratory channel; *L* – the length of riverbed subjected to lateral erosion; l_{u1}, l_{u2} – the length of reinforcements

that is, with the current inflow of bed load transport from the upper station towards the lower station, participating in the process of forming local pockets of lateral erosion below the damming structure. A total T_c time of 8 hours (28800 s) was adopted as sufficient to form a stable shape of a local lateral erosion pocket. The time, at which the changes in the shape of the riverbed occurred, and when the bed load movement in the area of lateral erosion was visually observed, was designated as T_r and it ranged from 1 hour to 6 hours.

The subject of comparative research was the volume of local lateral erosion V (volume of sand displaced downwards in the test section with a bottom that can be washed away – i.e. subject to lateral erosion), as well as geometrical parameters of the pothole: length of lateral erosion pocket L_s, distance of the point with the greatest depth from the end of bottom reinforcements (L_1) as well as maximum and average depth of the lateral erosion pocket, respectively: z_{max} and z_m (see: Fig. 3).

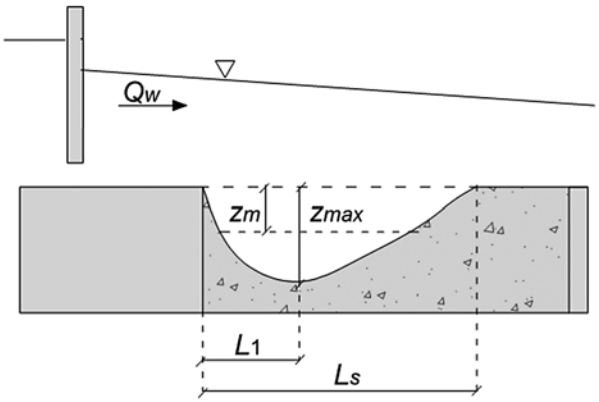

Fig. 3. Measured geometric parameters of local pockets of lateral erosion, where: Q_w – flow rate, z_m – average depth of the lateral erosion pocket; z_{max} – maximum depth of the lateral erosion pocket; L_s - length of the lateral erosion pocket; L_1 – distance from the deepest point to the end of the reinforcements

The characteristic of the depth of the lateral erosion pocket z_{max} and z_m was determined in relation to the initial height position of the bottom on the section of the riverbed that was subject to lateral erosion (see: Fig. 4). The average depth was estimated as the mean bottom position within the pothole (local

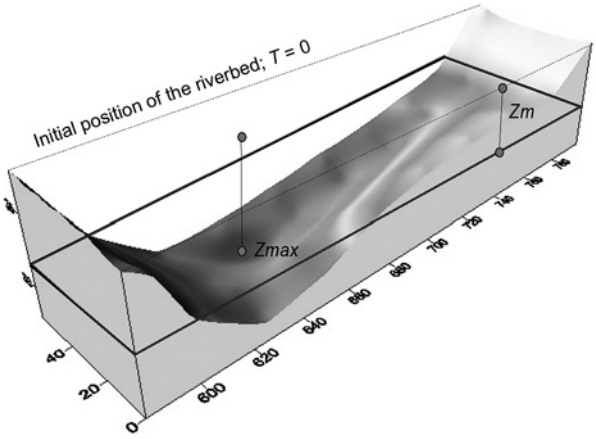

Fig. 4. Maximum depth z_{max} and average depth z_m of the local lateral erosion pocket

lateral erosion) with the average length of L_s, while the maximum depth of the lateral erosion pocket was determined as the lowest point in the accepted measurement grid.

Studies using a disc probe were carried out with the assumption of a measuring grid between 5 × 7 cm and 10 × 20 cm (see: Fig. 5).

It should be emphasized that carrying out the measurement of the channel with the length of 220 cm took the researcher approximately 25 minutes, while the automatic scanner measurement lasted from 7 to 10 minutes and only required the researcher's supervision in the event of a device failure. In addition, automatic control of the laser displacement along the laboratory channel allows for a significant compaction of the measurement grid. Laser scanning of the riverbed in comparative tests was carried out in a 10 mm × 10 mm measuring grid, with the accuracy of individual measuring points up to 0.1 mm. The coordinates of the *x, y* points and the height of *z* were measured with an accuracy of down to 0.5 mm. The development of measurement results obtained in the form of a point cloud was carried out based on the kriging method, based on the following assumptions:

– each value of the grid node is based on known points adjacent to the node,
– each point is assigned a weight expressed by its distance from the node; in this way, points further from the node will have less weight in estimating the value in the node.

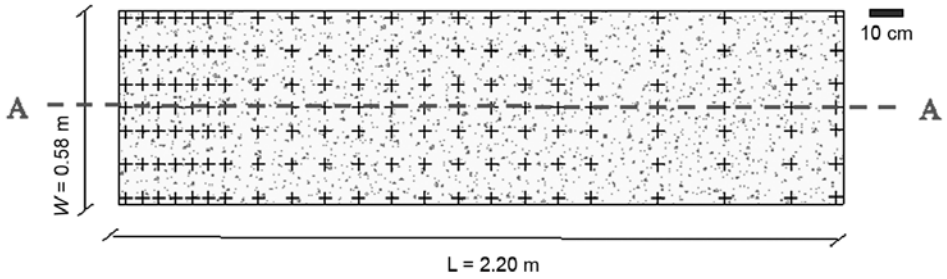

Fig. 5. Disc measurement grid for determining the shape of sandy river bed

LASER SCANNING TECHNOLOGY

LiDAR (Light Detection and Ranging) belongs to the group of active remote sensing systems that use electromagnetic radiation sent by the emitter. The result is a cloud of measurement points with three coordinates (*x, y, z*). The system consists of a transmitter, that is the module generating laser light (diodes), an optical telescope concentrating the returning reflected radiation, and a detector that converts light energy into an impulse stored in the module that registers the acquired data (see: Fig. 6). The cloud of points obtained in this way is then combined to create a 3D representation of the target object or area (Wehr and Lohr, 1999).

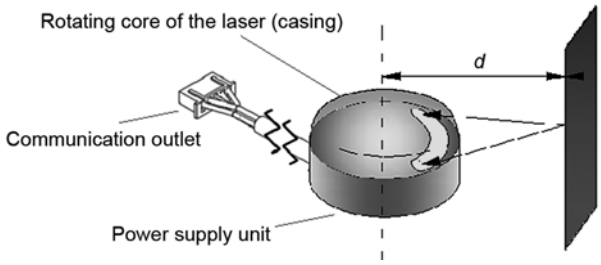

Fig. 6. Work schematics of RPLIDAR A2, where: *d* – distance between the emission unit and the reflexive surface

Data obtained by means of LiDAR technology, in the form of a point cloud, can be used to map terrain (see: Fig. 7), enabling observers to precisely indicate structures or areas of interest. Features and objects can be classified and extracted. Objects mapped using LiDAR technology can also be applied to visualize changes and anomalies, such as surface degradation (Jaboyedoff et al., 2010), or changes in slope gradient (Gordon et al., 2001).

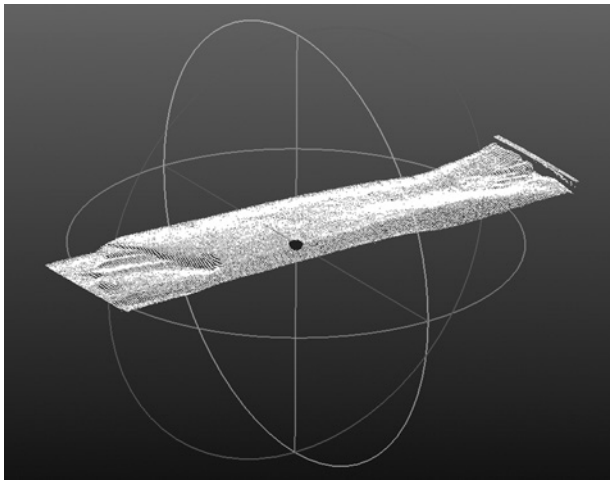

Fig. 7. A sample point cloud obtained using the LiDAR technology

The problem of using laser transmitters with a wavelength of about 785 nm, as used in this laboratory measurement device, is the lack of penetration of waves under the surface of the water. In this case, it is necessary either to perform additional bathymetric measurements using the echo sounder (Smart et al., 2009) or to remove the water from the area under examination. In laboratory conditions, during the measurement of the initial and final bottom position, the water flow was switched off, which enabled the measurement to be made on the "dry riverbed".

The use of LiDAR technology in the measurement of the shape and volume of the lateral erosion *f* the bottom of the laboratory channel is based on the introduction of an automatic measurement module, which, located above the channel bottom on a specially prepared control guide system, describes its shape by means of a point cloud. The prototype of the device

was constructed on the basis of autonomous elements, assembled into one system, controlled by means of commands, issued in a digital format. The prototype consists of a support frame, stepper motors, laser rangefinder, and control equipment (see: Fig. 8).

The RPLIDAR A2 360 laser rangefinder, rotating around the optical axis, performs up to 4,000 measurements per second with an angle accuracy of 0.9° and a distance of up to 0.5 mm, provided that the tested surface is no further than 1.5 m. The portable Raspberry Pi 3 computer enables the researcher to control the motion of stepper motors and to receive, digitize and store the data transmitted by the sensors. The computer also performs an initial analysis of the measurement results, which consists in eliminating those measurement results, which – for various reasons, are subject to a substantial measurement error. Step motors together with their controllers are used for precise movement of the device in the tested area. The graphic interface makes it easier for the operator to control the execution of the measurement series. The use of precision stepper motors in conjunction with dedicated controllers makes it possible to fix the motor in the desired position, and it reduces the vibrations of the entire system (see: Fig. 9).

The prototype (see: Fig 10) has the ability to move the LiDAR platform also across the channel, in order to check the areas potentially shielded from the optical axis of the sensor. The experiments carried out have shown that the nature of sand erosion in the laboratory channel does not require additional measurements with moving the LiDAR to other positions than in the middle of the examined station, taking into account the shape of the lateral erosion pocket (the point with the maximum depth is not obscured by the bottom elevation (see: Fig. 11). A beam of light reflects from the surface of the sandy bottom at an angle of 80 degrees – and a span of –40 to +40° is assumed.

As a result of the processing of digital results, the assumed geometrical parameters of local lateral erosion are obtained, including the volume of the local lateral erosion of the riverbed (see: Fig. 12).

Point cloud filtering consists in removing duplicate points and extreme outliers (accidentally read) using the SOR (Statistical Outlier Removal) filter with the following parameters: number of points used to estimate the average distance is 6, whereas the standard deviation multiplier threshold is 1.00.

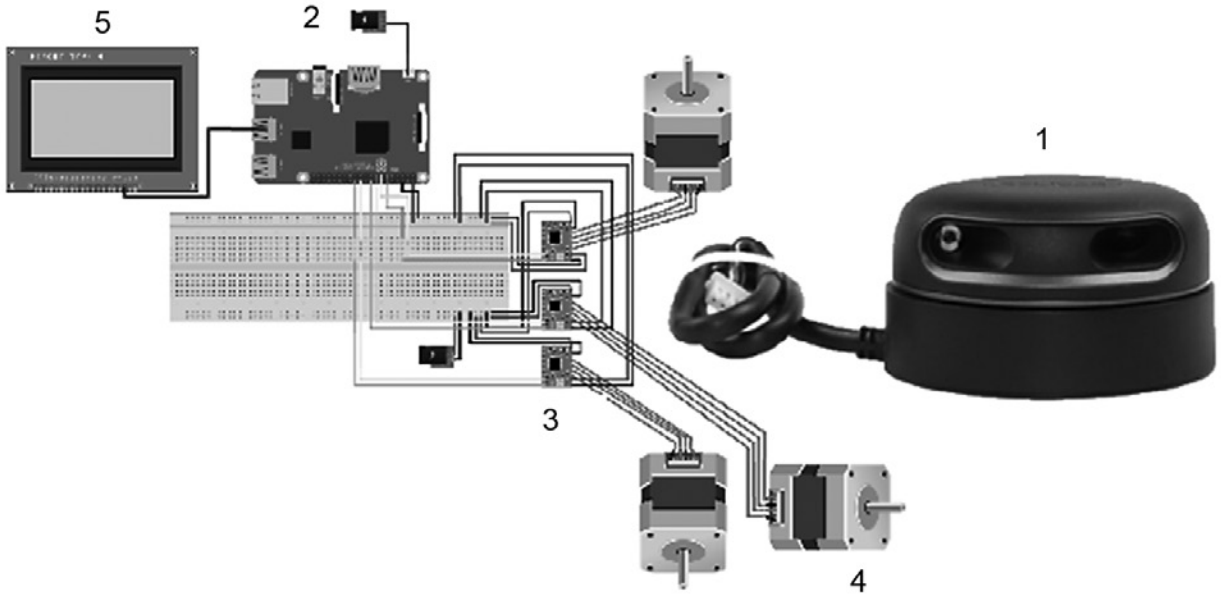

Fig. 8. Schematics of the device: 1 – RPLIDAR A2 laser rangefinder; 2 – Steering computer; 3,4 – Controllers of stepped motors, and stepped motors; 5 – screen and steering units

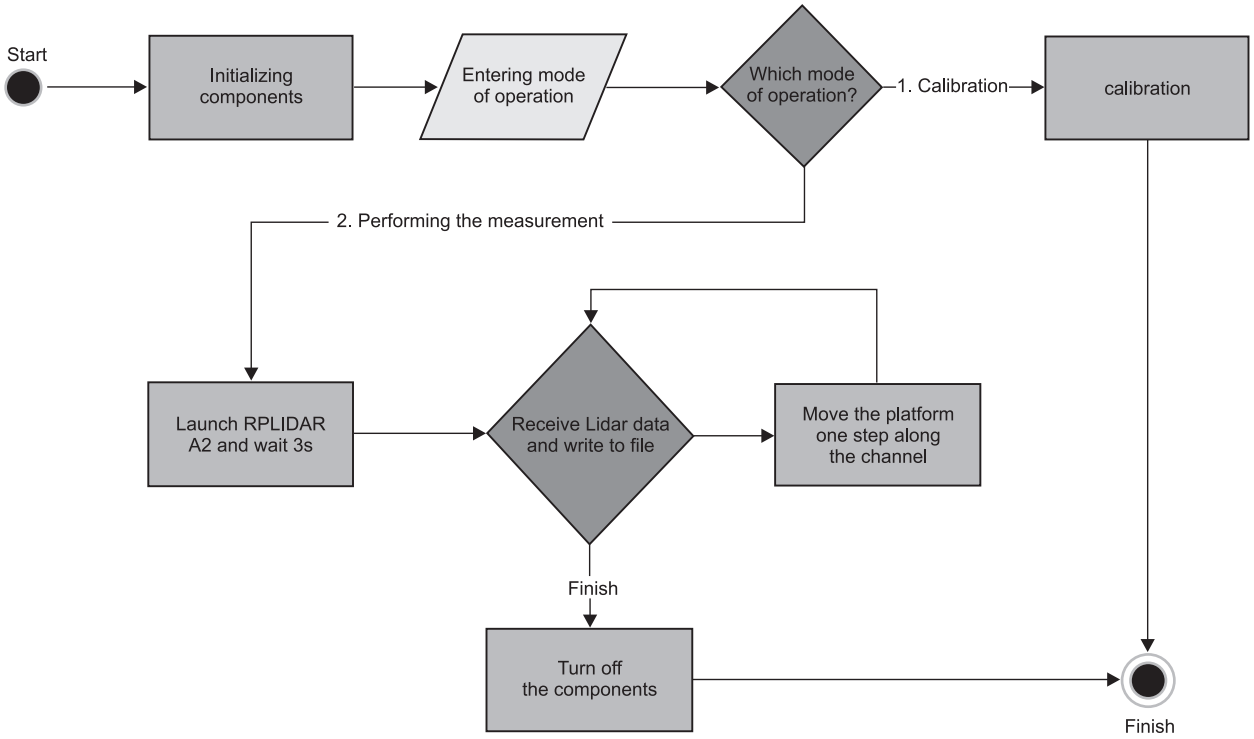

Fig. 9. Work schematics of the device prototype

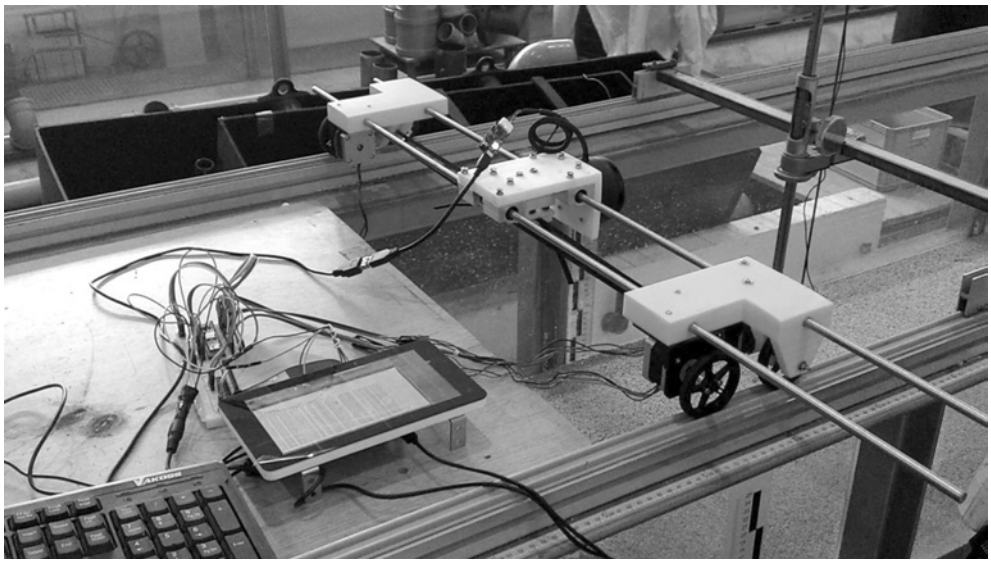

Fig. 10. Prototype of the device during operation at the laboratory (photo by M. Kiraga)

Fig. 11. Working schematics of the laser unit

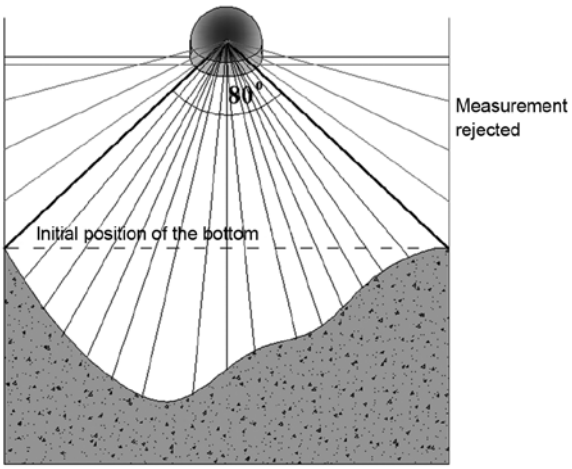

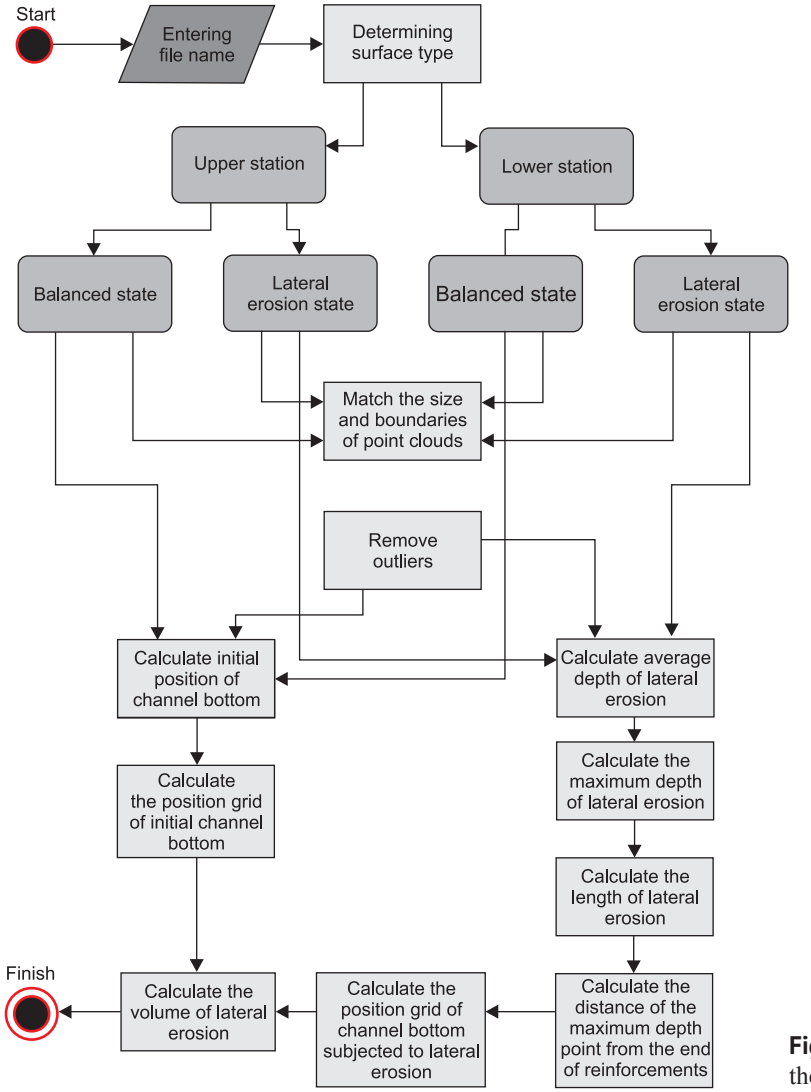

Fig. 12. Diagram of processing digital data to the required data format

RESULTS AND DISCUSSION

The result of the research was obtaining clouds of points (*x, y, z*), reflecting the location of the bottom before and after the formation of local lateral erosion in twenty series of measurements with different hydraulic conditions. The subject of the study was the basic geometrical parameters of the potholes and their volume. The study aimed at comparing the results of tests carried out using two methods – the traditional method, using a disc probe and producing lower accuracy, and the laser scanning technology.

Applications of LiDAR technology to bathymetric measurements have been used and developed for a long time (including Enabnit, 1980; Guenther, 1985; Mandlburger et al., 2015), and its reliability has been confirmed in numerous studies (Kinzel et al. 2007; Peeri and Philpot, 2007; Kotilainen and Kaskela, 2017), however, devices used in riverbed morphology studies can not be used in relatively simple laboratory tests due to the considerations of measurement accuracy, as well as the size, weight and price of the device. The aforementioned factors were the reason for undertaking work on the independent construction of the device based on prefabricated elements, in which we were guided by the principle of minimizing the size and costs with the best possible reading accuracy.

Measurement with the use of a scanner allowed us to obtain, in a shorter time, a much more accurate riverbed height mapping on the lateral erosion section, compared to the one determined on the basis of the measurement made using the probe (see: Fig. 13).

The use of a laser scanner allowed for relatively fast processing of data into the graphic format (see: Fig. 14). The traditional methodology required the researcher to entered the studied coordinates manually.

Table 2 presents the results of comparative tests, that is the values of the analysed geometric parameters determined by the use of two methods, as well as the relative errors obtained (the result of comparing one method against the other, with a much denser measurement grid). The relative errors obtained range from 0 to 95%. Thus: in the case of the average depth of the lateral erosion, the errors ranged from approx. 0 to 69%; for the maximum depth of the lateral erosion, from approx. 0 to 52%; for the lateral erosion length – from approx. 0 to 52%; for the distance of the point with the greatest depth from the end of bottom reinforcements from approx. 0 up to 46%; and for the volume of lateral erosion from 1 to 95%.

Accurate estimation of the above described geometrical properties of local lateral erosion is important due to the fact that empirical equations, binding these parameters to the granulometric and hydraulic conditions of riverbeds, ultimately applicable to natural conditions and, in general, applied in estimating transport of bedload, are formulated and pre-verified on the basis of laboratory tests.

The analysis of the obtained results indicates an increase in the size of the lateral erosion, characterized by its length, volume and depth as the increase in the unit flow rate (see: Fig. 15–17) of the velocity of flowing water (see: Fig. 18–20). The local length of the lateral erosion pocket does not exceed 2.20 m, because it covers the entire length of the sandy basin.

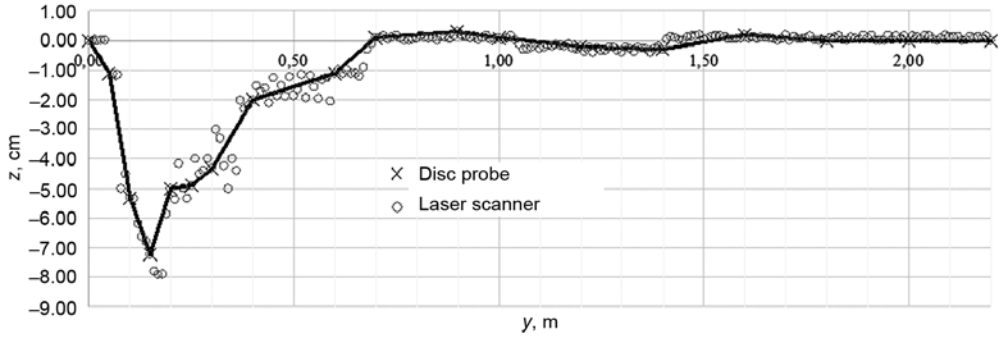

Fig.13. Sample shape of the longitudinal section of the alluvial riverbed (A–A section at the riverbed axis), where: z – depth; y – distance

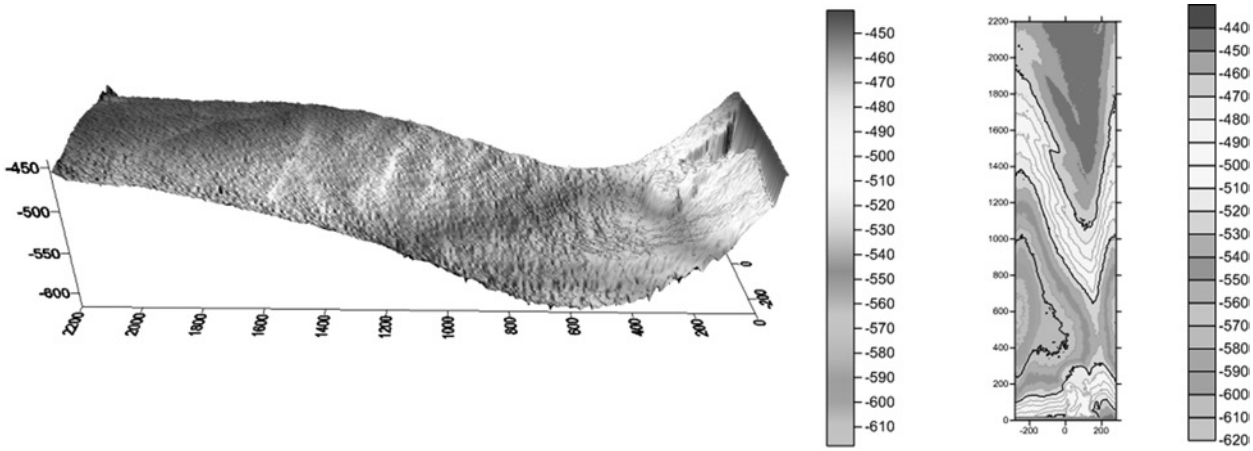

Fig. 14. 3D image and the map of the riverbed shape subjected to lateral erosion; all measurements given in [mm]

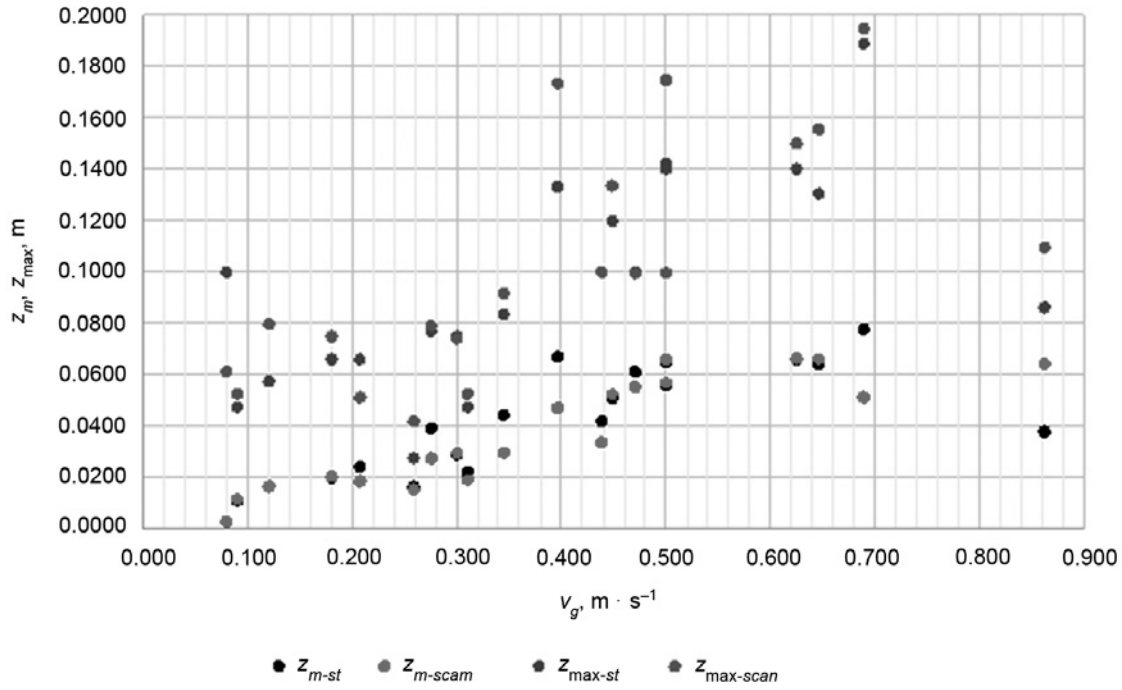

Fig. 15. Correlation of typical depths of local lateral erosion pockets (average z_m and maximum z_{max}) in the conditions of water flow described by the velocity of v_g in the upper station of the structure; where: $z_{m\text{-}st}$ – average depth of the local lateral erosion pocket determined using the disc probe; $z_{m\text{-}scan}$ – average depth of the local lateral erosion pocket determined using the laser scanning method; $z_{max\text{-}st}$ – maximum depth of the local lateral erosion pocket determined using the disc probe; $z_{max\text{-}scan}$ – maximum depth of the local lateral erosion pocket determined using the laser scanning method.

Table 2. Results of laboratory measurements using disc probe and laser scanning method

No. of measurement series	$z_{m\text{-}st}$	$z_{m\text{-}scan}$		$z_{\max\text{-}st}$	$z_{\max\text{-}scan}$		$L_{s\text{-}st}$	$L_{s\text{-}scan}$		$L_{1\text{-}st}$	$L_{1\text{-}scan}$		V_s	V_{scan}	
	[m]	[m]	[%]	[m]	[m]	[%]	[m]	[m]	[%]	[m]	[m]	[%]	[m^3]	[m^3]	[%]
1	0.0393	0.0275	30.0	0.0770	0.0790	2.6	1.20	0.91	24.2	0.50	0.55	10.0	0.00800	0.01258	57.3
2	0.0442	0.0296	33.0	0.0834	0.0916	9.8	2.10	1.77	15.7	0.30	0.31	3.3	0.03000	0.04324	44.1
3	0.0777	0.0513	34.0	0.1888	0.1945	3.0	2.10	2.20	4.8	0.80	0.80	0.0	0.07600	0.07279	4.2
4	0.0166	0.0154	7.2	0.0275	0.0418	52.0	0.50	0.37	26.0	0.20	0.22	10.0	0.00140	0.00162	15.7
5	0.0670	0.0471	29.7	0.1333	0.1731	29.9	2.20	2.20	0.0	0.65	0.56	13.8	0.06300	0.06839	8.6
6	0.0221	0.0193	12.7	0.0475	0.0525	10.5	0.70	0.71	1.4	0.20	0.16	20.0	0.00250	0.00417	66.8
7	0.0241	0.0187	22.4	0.0660	0.0513	22.3	0.60	0.70	16.7	0.25	0.22	12.0	0.00120	0.00151	25.8
8	0.0641	0.0661	3.1	0.1305	0.1555	19.2	2.20	2.20	0.0	0.70	0.61	12.9	0.11220	0.11336	1.0
9	0.0379	0.0641	69.1	0.0862	0.1095	27.0	2.00	2.20	10.0	0.60	0.61	1.7	0.11000	0.11106	1.0
10	0.0610	0.0553	9.3	0.0999	0.0995	0.4	2.20	2.20	0.0	0.60	0.79	31.7	0.07000	0.07299	4.3
11	0.0420	0.0338	19.5	0.1000	0.1000	0.0	2.20	2.20	0.0	0.50	0.27	46.0	0.06700	0.05227	22.0
12	0.0510	0.0524	2.7	0.1197	0.1334	11.4	2.20	2.20	0.0	0.60	0.79	31.7	0.06900	0.07178	4.0
13	0.0661	0.0662	0.2	0.1401	0.1500	7.1	2.20	2.20	0.0	0.65	0.62	4.6	0.09900	0.10225	3.3
14	0.0165	0.0167	1.2	0.0575	0.0798	38.8	0.80	0.88	10.0	0.30	0.37	23.3	0.00340	0.00408	20.0
15	0.0028	0.0029	3.6	0.1000	0.0613	38.7	0.60	0.68	13.3	0.30	0.22	26.7	0.00220	0.00351	59.5
16	0.0201	0.0205	2.0	0.0660	0.0749	13.5	0.70	0.70	0.0	0.20	0.22	10.0	0.00290	0.00364	25.5
17	0.0560	0.0568	1.4	0.1401	0.0997	28.8	2.00	1.77	11.5	0.35	0.31	11.4	0.04200	0.04324	3.0
18	0.0110	0.0115	4.5	0.0475	0.0525	10.5	0.70	0.72	2.9	0.20	0.17	15.0	0.00200	0.00390	95.0
19	0.0290	0.0294	1.4	0.0750	0.0742	1.1	1.10	0.93	15.5	0.40	0.27	32.5	0.00900	0.01258	39.8
20	0.0650	0.0657	1.1	0.1420	0.1746	23.0	2.20	2.20	0.0	0.65	0.58	10.8	0.06400	0.06999	9.4

where: $z_{m\text{-}st}$ – average depth of the local lateral erosion pocket determined using the disc probe; $z_{m\text{-}scan}$ – average depth of the local lateral erosion pocket determined using the laser scanning method; $\delta_{x\text{-}zm}$ – relative error of observation for average depth; $z_{\max\text{-}st}$ – maximum depth of the local lateral erosion pocket determined using the disc probe; $z_{m\text{-}scan}$ – maximum depth of the local lateral erosion pocket determined using the laser scanning method; $\delta_{x\text{-}zmax}$ – relative error of observation for maximum depth; $L_{s\text{-}st}$ – length of lateral erosion pocket determined using the disc probe; $L_{s\text{-}scan}$ length of lateral erosion pocket determined using the laser scanner; $\delta_{x\text{-}Ls}$ – relative error of observation for the length of the lateral erosion; $L_{1\text{-}st}$ – the distance from the deepest point to the end of the reinforcements determined using the disc probe; $L_{1\text{-}scan}$ – the distance from the deepest point to the end of the reinforcements determined using the laser scanner; $\delta_{x\text{-}Ls}$ – relative error of observation for the distance from the deepest point to the end of the reinforcements; V_s – volume of the lateral erosion pocket determined using the disc probe; V_{scan} – volume of the lateral erosion pocket determined using the laser scanner; $\delta_{x\text{-}V}$ – relative error of observation for the volume of lateral erosion

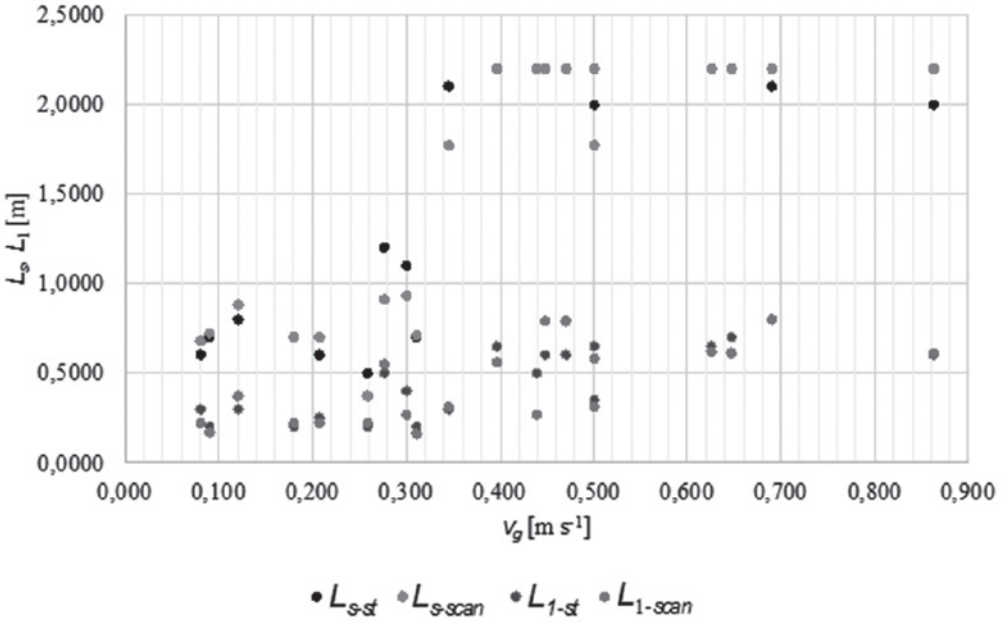

Fig. 16. Correlation of typical lengths of local lateral erosion pockets (total length of L_s and the distance from the deepest point to the end of the reinforcements L_1) in the conditions of water flow described by the velocity of v_g in the upper station of the structure; where: $L_{s\text{-}st}$ – total length of lateral erosion pocket determined using the disc probe; $L_{s\text{-}scan}$ – total length of lateral erosion pocket determined using the laser scanning method; $L_{1\text{-}st}$ – the distance from the deepest point to the end of the reinforcements determined using the disc probe; $L_{1\text{-}scan}$ – the distance from the deepest point to the end of the reinforcements determined using the laser scanning method.

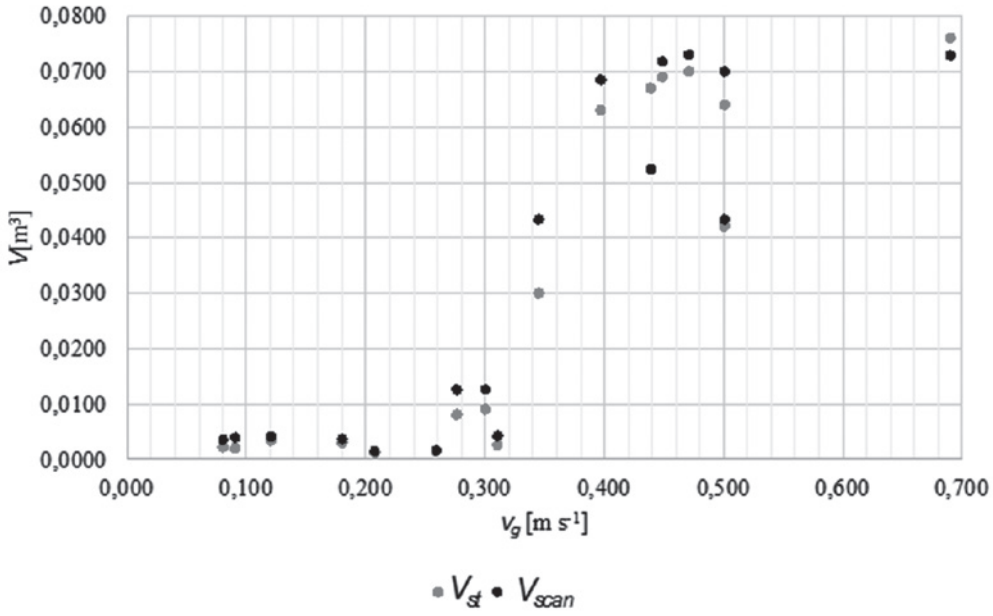

Fig. 17. Correlation of local lateral erosion volume V, described by velocity v_g in the upper station of the structure; where: V_{st} – volume of the lateral erosion pocket determined using the disc probe; V_{scan} – volume of the lateral erosion pocket determined using the laser scanning method.

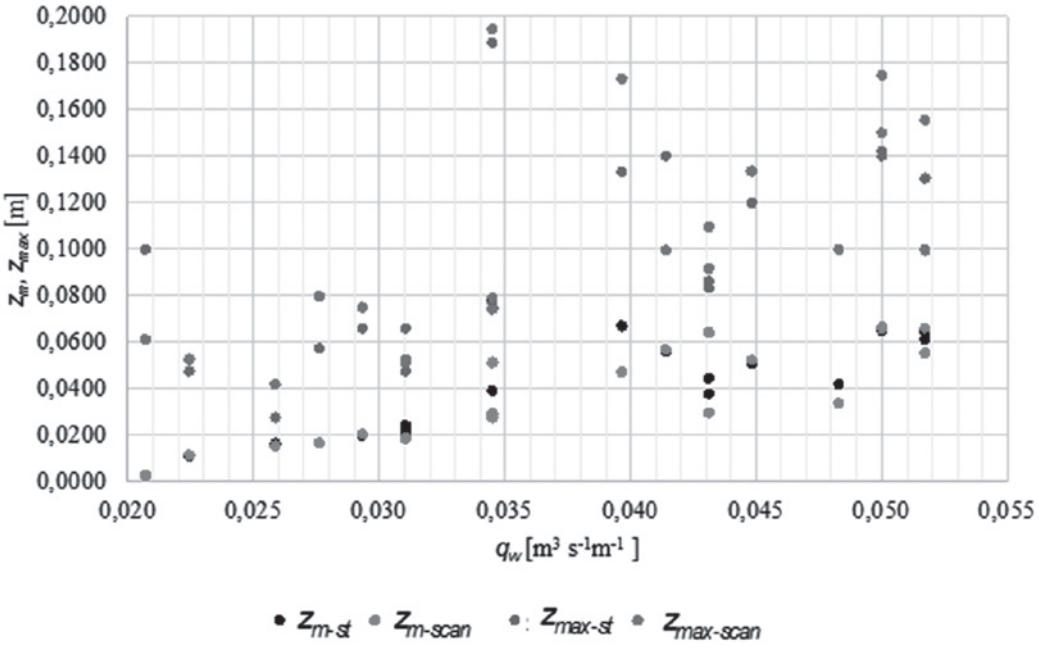

Fig. 18. Correlation of typical depths of local lateral erosion pockets (average z_m and maximum $z_{\max}$) in the conditions of water flow described by unit flow rate of q_w

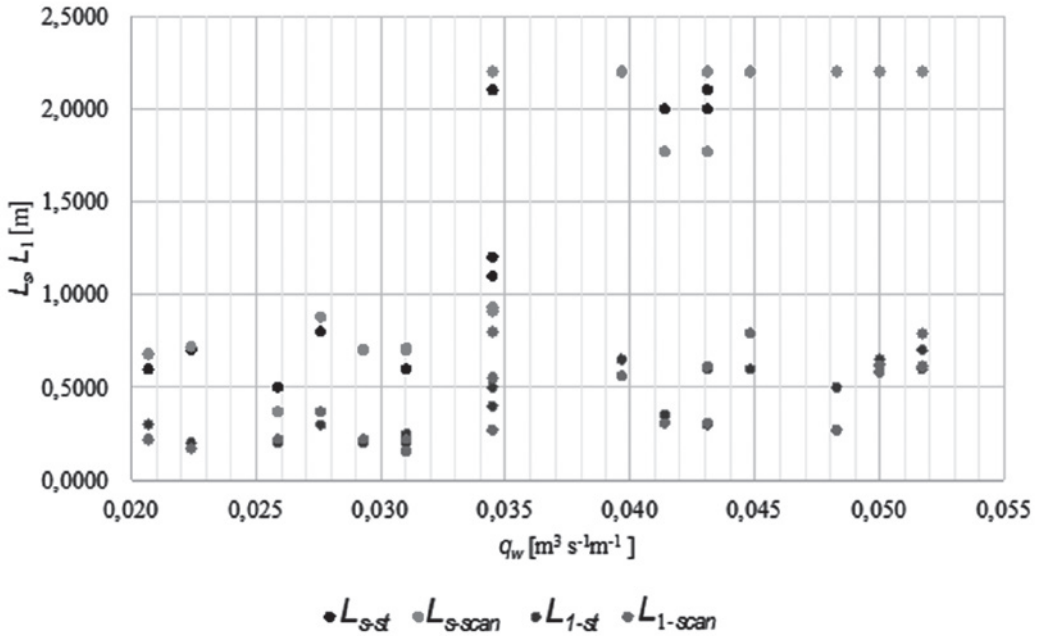

Fig. 19. Correlation of typical lengths of local lateral erosion pockets (total length of L_s and the distance from the deepest point to the end of the reinforcement L_1) in the conditions of water flow described by unit flow rate of q_w

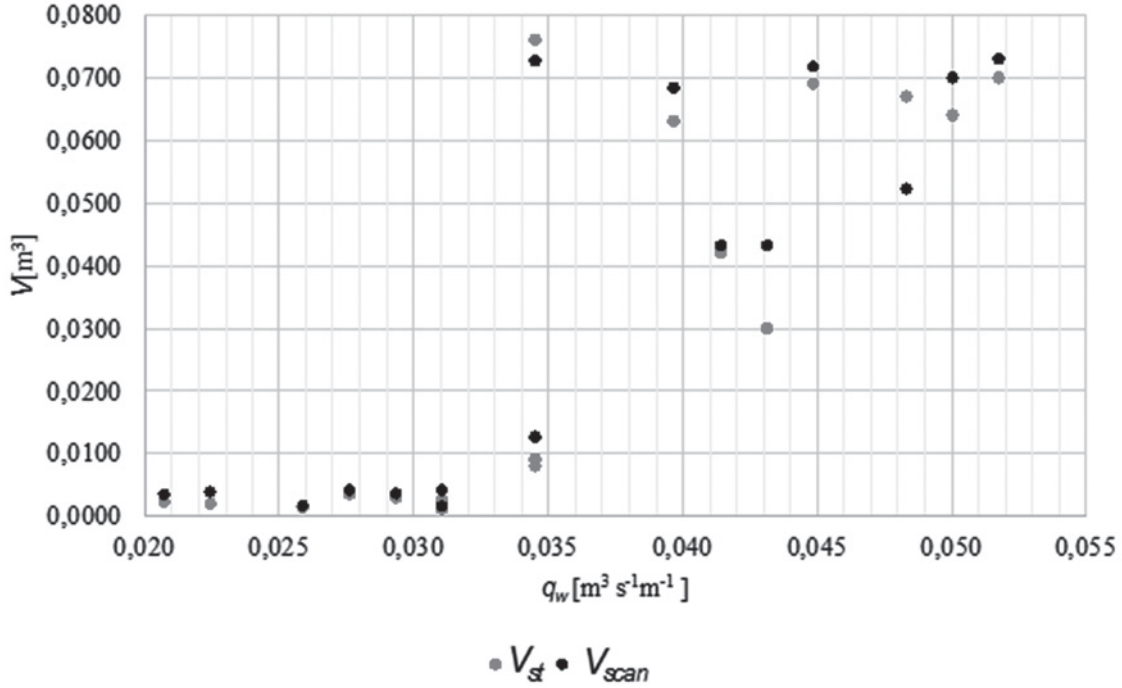

Fig. 20. Correlation of local lateral erosion volumes V, flow described by unit flow rate of q_w

CONCLUSIONS

The device constructed using LiDAR technology, a portable computer, precision stepper motors and dedicated software makes it possible to automate work in laboratory conditions. The result is high accuracy of measurements and their significant acceleration. The assumed coordinate grid is characterized by high density. In combination with high accuracy this allows for a precise description of the shape of the analysed surface, which can be presented graphically or numerically. The obtained coordinates can be transformed into a volume of the local lateral erosion pocket, based on the known location of the riverbed before its formation.

On the basis of the obtained data, it is also possible to define other characteristic parameters of lateral erosion, such as its length and maximum depth. However, we must not fail to mention the fact that the constructed prototype has been checked in the absence of water in the channel – the disadvantage of using LiDAR devices is the impossibility of using them during the water flow.

When applying the method of manually measuring the bottom position, the same accuracy as for an automatic device equipped with a laser will not be achieved. It was found that the relative error in relation to the values of the channel lateral erosion parameters, determined on the basis of the hand-held disc probe and by laser scanner measurements was from 0 to approx. 95%, with the average error values being as follows: for the estimation of maximum depth, 17.5%; for the estimation of average depth, 14.4%; for the distance of the point with maximum depth from the end of reinforcements, 16.4%; for the total length of lateral erosion, 7.6%; and for its volume, 25.5%.

REFERENCES

Bajkowski, S., Siwicki, P., Urbański, J. (2002). *Wykorzystanie badań laboratoryjnych rozmyć poniżej budowli wodnych do oceny ich bezpieczeństwa*. Acta Scientiarum Polonorum, 1–2, 41–51.

Bajkowski, S. (2010). *Współczesne techniki pomiarowe laboratoriów wodnych. Infrastruktura i ekologia terenów wiejskich*, 8(2), 37–50.

Baltsavias, E. (1999). *Airbone laser scanning: basic relations and formulas.* ISPRS J Photogramm Remote Sens, 54, 199–214.

Ben Meftah, M., Mossa, M. (2006). *Scour holes downstream of bed sills in low-gradient channels*. Journal of Hydraulic Research, 4(44), 497–509.

Besl, P., McKay, N. (1992). *A method for registration of 3-D shapes*. IEEE Trans Pattern Anal Mach Intell, 14, 239–256.

Błażejewski, R. (1989). *Prognozowanie rozmyć miejscowych gruntów niespoistych poniżej budowli upustowych.* Poznań: Wydawnictwo Akademii Rolniczej.

Breusers, H. C., Raudkivi, A. J. (1991). *Scouring: Hydraulic Structures Design Manual Series.* Balkema: I.A.H.R., Balkema.

Chabert, J., Engeldinger, P. (1956). *Etude des affouillements autour des piles des ponts. Study on scour around bridge piers.* Chatou, Francja: Laboratoire National d'Hydraulique.

Chividini, M. F. (1983). *Evaluation of maximumscour downstream of ski-jump spillways.* Proceedings of the 11th Water National Congress, 6, Cordoba, Argentyna, 187–210.

Clarke, F. W. (1962). *The Action of Submerged Jets on Moveable Material.* Praca magisterska. Londyn: Wydział Inżynierii Środowiska, Imprerial College.

Dąbkowski, S. L., Siwicki, P. (2000). *Analiza głębokości rozmycia koryta na modelach jazu.* Przegląd Naukowy Wydziału Inżynierii i Kształtowania Środowiska, 19, 39–50.

Enabnit, D., Nield, Van K. (1980). *Airborne Laser Hydrography.* International Hydrographic Review, 57(2), 93–99.

Gaudio, R., Marion, A., Bovolin, V. (2000). *Morphological effects of bed sills in degrading rivers.* Journal of Hydraulic Research, 38(2), 89–96.

Gordon, S., Lichti, D., Stewart, M. (2001). *Application of a high-resolution, ground-based laser scanner for deformation measurements.* In: *Proceedings of the 10th international FIG symposium on deformation measurements*, Orange, California, USA, 19–22 Marca 2001, 23–32.

Guenter, G. (1985). *Airborne Laser Hydrography*: System Desing and Perfomance Factors. USA.

Haneberg, W. (2007). *Directional roughness profiles from three-dimensional photogrammetric or laser scanner point clouds.* In: E. Eberhardt, D. Stead, T. Morrison, (eds.), *Rock mechanics: meeting society's challenges and demands.* Proceedings of the 1st Canada–US rock mechanics symposium, Vancouver, Canada, 27–31 Maja, 2007, Taylor & Francis, 101–106.

Jaboyedoff, M., Oppikofer, T., Abella´n, A., Derron, M., Loye, A., Metzger, R., Pedrazzini, A. (2010). Use of LIDAR in landslide investigations: a review.Nat Hazards (2012) 61, 5–28.

Kaszowski, L., Kotarba, A., Nowak, W. (1970). *Wpływ katastrofalnych wezbrań na przebieg procesów fluwialnych*. Warszawa: PWN.

Kiraga, M., Popek, Z. (2016). *Using a modified Lane's relation in local bed scouring studies in alluvial bed. Acta Scientarum Polonorum Formatio Circumiectus*, 15(4), 209–226.

Kiraga, M., Popek, Z. (2016). *Using a modified Lane's relation in local bed scouring studies in the laboratory channel*. Water, 8(16), 1490–1509.

Kiraga, M., Popek, Z. (2018). *Geometry Description of Local Scouring Process in Various Laboratory Water Structure Models.* In: M. B. Kalinowska, M. M. Mrokowska, P. M. Rowiński (eds.) Free Surface Flows and Transport Processes. Springer, 245–258.

Kinzel, P., Wright, W., Nelson, J., Burman, A. (2007). *Evaluation of an Experimental LiDAR for Surveying a Shallow, Braided, Sand-Bedded River*, Journal of Hydraulic Engineering, 133, 7.

Kotilainen, A., Kaskela, A. (2017), *Comparison of airborne LiDAR and shipboard acoustic data in complex shallow water environments*: Filling in the white ribbon zone, Marine Geology, 385, 250–259.

Lenzi, M. A., Marion, A., Comiti, F. (2003). *Local scouring at grade-control structures in alluvial mountain rivers.* Water Resources Research, 39(7), 1176–1188.

Novak, P., Moffat, A. I., Nalluri, C., Narayanan, R. (2006). Hydraulic Structures. London and New York: Taylor&Francis.

Mandlburger, G. Hauer, Ch., Wieser, M., Pfeifer, N. (2015). *Topo-Bathymetric LiDAR for Monitoring River Morphodynamics and Instream Habitats–A Case Study at the Pielach River.* Remote Sens. 7, 6160–6195.

Pagliara, S., Radecki-Pawlik, A., Palermo, M., Plesiński, K. (2017). *Block ramps in curved rivers: morphology analysis and prototype data supported design criteria for mild bed slopes.* River Research and Applications, 33(3), 427–437.

Peeri, S., Philpot, W. (2007), *Increasing the Existence of Very Shallow-Water LIDAR Measurements Using the Red-Channel Waveforms*, IEEE Transactions on Geoscience and Remote Sensing, 45, 5, 1217–1223.

Petts, G. E. (1977). *Channel response to flow regulation: the case of the River Derwent, Derbyshire*. in: K.J Gregory (ed.), *River channel changes Chichester Wiley. Chichester*: John Wiley and Sons, 145–164.

Smart, G., Bind, J., Duncan, M. (2009). *River bathymetry from conventional LiDAR using water surface returns.* 18th World IMACS / MODSIM Congress, Cairns, Australia 13–17 July 2009.

Ślizowski, R., Radecki-Pawlik, A. (2003). *Weryfikacja formuł do obliczania rozmycia nieumocnionego dna poniżej budowli wodnej na podstawie pomiarów laboratoryjnych*. Acta Scientiarium Polonorum Formatio Cirtumiectus, 3(3), 25–34.

Urbański, J. (2005). *Rozwój miejscowego rozmycia w czasie na modelach jazu w dwóch skalach.* Przegląd Naukowy Inżynieria i Kształtowanie Środowiska, 1(31), 67–75.

Urbański, J., Hejduk, L. (2014). *The analysis of local scour size formed after flood event.* Monografie Komitetu Gospodarki Wodnej PAN, 20, 389–400.

Wehr, A., Lohr, U. (1999). *Airborne laser scanning–an introduction and overview.* ISPRS J Photogramm Remote Sens, 54, 68–82.

Wierzbicki, M., Hämmerling, M. (2011). *Wpływ budowy progów stabilizujących na kształtowanie się układu zwierciadła wody i dna poniżej zbiornika Jeziorsko.* Gospodarka Wodna, 6, 239–243.

WYKORZYSTANIE TECHNOLOGII SKANINGU LASEROWEGO W BADANIACH UKSZTAŁTOWANIA DNA ALUWIALNEGO W WARUNKACH LABORATORYJNYCH

ABSTRAKT

Praca badawcza ma na celu porównanie wyników ukształtowania dna piaszczystego w warunkach laboratoryjnych otrzymanych metodą tradycyjną oraz z użyciem autorskiego rozwiązania, opierającego się na technologii LiDAR.

Zastosowanie technologii LiDAR w pomiarach kształtu i objętości rozmycia dna koryta laboratoryjnego opiera się na wprowadzeniu automatycznego modułu pomiarowego, który umieszczony powyżej dna koryta na specjalnie przegotowanym sterowalnym układzie prowadnic, opisuje jego kształt za pomocą chmury punktów.

Efektem przeprowadzonych badań było otrzymanie chmur punktów (x, y, z), odzwierciedlających położenie dna przed i po uformowaniu się lokalnego rozmycia w dwudziestu seriach pomiarowych o zróżnicowanych warunkach hydraulicznych. Przedmiotem badania były podstawowe parametry geometryczne wybojów oraz jego objętość. Pomiar z użyciem skanera pozwolił na uzyskanie w krótszym czasie znacznie dokładniejszego odwzorowania wysokościowego dna na odcinku rozmycia, w porównaniu z określonym na podstawie pomiaru wykonanego sondą, a także na stosunkowo szybkie przetwarzanie danych do formy graficznej. Urządzenie wyposażone w przenośny komputer, precyzyjne silniki krokowe oraz specjalne oprogramowanie pozwala na zautomatyzowanie pracy w warunkach laboratoryjnych. Efektem jest nie tylko duża dokładność pomiarów, ale i ich znaczne przyspieszenie. Założona siatka współrzędnych cechuje się dużą gęstością, co w połączeniu z dużą dokładnością pozwala na precyzyjny opis kształtu analizowanej powierzchni, która może być przedstawiona w sposób graficzny lub numeryczny. Stosując metodę ręcznego pomiaru położenia dna, trudno osiągnąć taką samą dokładność jak w przypadku automatycznego urządzenia wyposażonego w laser.

Słowa kluczowe: skaning laserowy, lokalne rozmycia, pomiary dna, budowle wodne, interpolacja powierzchni